Phosphoregulation of the transcription factor Mxr1 plays a crucial role in the concentration-regulated methanol induction in *Komagataella phaffii*

Running title: Phosphoregulation of KpMxr1

Koichi Inoue[1], Shin Ohsawa[1], Shinji Ito[2], Hiroya Yurimoto[1,*], and Yasuyoshi Sakai[1]

[1] *Division of Applied Life Sciences, Graduate School of Agriculture, Kyoto University, Kitashirakawa-Oiwake, Sakyo-ku, Kyoto 606-8502, Japan.*
[2] *Medical Research Support Center, Graduate School of Medicine, Kyoto University, Yoshida Konoe-cho, Sakyo-ku, Kyoto 606-8501, Japan.*

*Correspondence: Hiroya Yurimoto, Ph.D.
Associate Professor
Division of Applied Life Sciences, Graduate School of Agriculture, Kyoto University, Kitashirakawa-Oiwake, Sakyo-ku, Kyoto 606-8502, Japan. Tel.: +81 75 753 6387; fax: +81 75 753 6454;
e-mail: yurimoto.hiroya.5m@kyoto-u.ac.jp

Data availability statement

The data that support the findings of this study are available in the supplementary material of this article.

Funding statement

This research was supported in part by Grant-in-Aid for Scientific Research on Innovative Areas (19H05709 to YS), Grant-in-Aid for Scientific Research (B) (19H04326 and 22H03802 to HY) and Grant-in-Aid for JSPS Fellows (19J21821 to KI) from the Japan Society for the Promotion of Science. This research was also supported in part by grants from the Institution of Fermentation, Osaka (IFO) and Noda Institute of Scientific Research to HY.

Conflict of interest disclosure

The authors declare no conflicts of interest.

Abstract

Methylotrophic yeasts can utilize methanol as the sole carbon and energy source and the expression of their methanol-induced genes is regulated based on the environmental methanol concentration. Our understanding of the function of transcription factors and Wsc family of proteins in methanol-induced gene expression and methanol sensing is expanding, but the methanol signal transduction mechanism remains undetermined. Our study has revealed that the transcription factor KpMxr1 is involved in the concentration-regulated methanol induction (CRMI) in *Komagataella phaffii* (*Pichia pastoris*) and that the phosphorylation state of KpMxr1 changes based on methanol concentration. We identified the functional regions of KpMxr1 and determined its multiple phosphorylation sites. Non-phosphorylatable substitution mutations of these newly identified phosphorylated threonine and serine residues resulted in significant defects in CRMI. We revealed that KpMxr1 receives the methanol signal from Wsc family proteins via KpPkc1 independent of the mitogen-activated protein kinase (MAPK) cascade and speculate that the activity of KpPkc1 influences KpMxr1 phosphorylation state. We propose that the CRMI pathway from Wsc to KpMxr1 diverges from KpPkc1 and that phosphoregulation of KpMxr1 plays a crucial role in CRMI.

Keywords: methylotrophic yeast, transcription factor, signal transduction, gene regulation, phosphoregulation

1 INTRODUCTION

Methylotrophic yeasts, such as *Komagataella phaffii* (synonym *Pichia pastoris*), *Ogataea polymorpha* (synonym *Hansenula polymorpha*), and *Candida boidinii,* can utilize methanol as the sole source of carbon and energy. During growth on methanol, these yeasts develop large peroxisomes containing copious amounts of methanol metabolizing enzymes such as alcohol oxidase (AOX) and dihydroxyacetone synthase (DAS), whose gene expression is strongly induced by methanol. Owing to their strong methanol-induced gene promoters, methylotrophic yeasts have been used as hosts for recombinant protein production (Cregg *et al.*, 2000; Gellissen, 2000; Yurimoto, 2009). Their unique one-carbon (C1) metabolism and the molecular mechanism for methanol-induced gene expression have been extensively studied for more than 50 years (De *et al.*, 2021; Hartner *et al.*, 2006; Kalender *et al.*, 2020; Klei, van der *et al.*, 2006; Ogata *et al.*, 1969; Yurimoto *et al.*, 2011; Yurimoto *et al.*, 2019) (Figure S1a).

One of the main habitats of methylotrophic yeasts in nature is the phyllosphere, the aerial portions of plants. They utilize the methanol that is generated from the methyl ester group of the cell wall component pectin on plant leaves (Kawaguchi *et al.*, 2011). Methanol concentration in the phyllosphere exhibits a daily periodicity with a dynamic range of 0-0.2% (ca. 0-60 mM) (Kawaguchi *et al.*, 2011). Thus, methylotrophic yeasts must sense the presence and concentration of methanol and regulate the expression of methanol-induced genes and the metabolism of methanol based on that information. Formaldehyde generated from the oxidation of methanol by AOX is a key intermediate in the metabolism of methylotrophic yeasts, and is positioned at the branch point of the assimilatory and dissimilatory pathways (Figure S1a). Since formaldehyde is toxic to cells and unbalanced methanol metabolism results in the accumulation of formaldehyde,

80 expression levels of the formaldehyde-generating enzyme, AOX, and formaldehyde-
81 consuming enzymes, DAS and formaldehyde dehydrogenase (FLD), should be properly
82 controlled according to environmental methanol concentrations. Indeed, in a previous
83 study we found that the transcript levels of AOX- and DAS-encoding genes increased in
84 the presence of 0.001-0.1% methanol but decreased in the presence of more than 0.1%
85 methanol (Figure 1a) (Ohsawa *et al.*, 2017). Consequently, elucidating the molecular
86 mechanism of concentration-regulated methanol induction (CRMI) is important not
87 only for understanding the adaptation mechanism of the yeasts to the phyllosphere
88 environment where methanol concentration changes periodically, but also to improve
89 the productivity of heterologous proteins generated from them.
90 In methylotrophic yeasts, methanol-induced gene expression is strictly regulated
91 depending on the carbon source (Yurimoto *et al.*, 2011; Yurimoto *et al.*, 2019). The
92 activation of methanol-induced genes undergoes two regulatory steps: the expression is
93 strongly repressed in the presence of glucose, but is activated to a certain level in the
94 absence of glucose (derepression), and it is substantially induced in the presence of
95 methanol depending on the methanol concentration, i.e., CRMI. A series of
96 transcription factors involved in methanol-induced gene expression have been identified
97 and characterized using *K. phaffii*, *C. boidinii* and *O. polymorpha* in previous studies.
98 Some of these transcription factors, such as the homologs of *Saccharomyces cerevisiae*
99 Adr1, KpMxr1 and CbTrm2, are involved in derepression (Lin-Cereghino *et al.*, 2006;
100 Sasano *et al.*, 2010). Three kinds of transcription factors are involved in methanol
101 induction; i) Mpp1 (HpMpp1 and KpMit1) (Leão-Helder *et al.*, 2003; Wang *et al.*,
102 2016), ii) Trm1 (CbTrm1 and KpTrm1) (Sasano *et al.*, 2008; Sahu *et al.*, 2014), and iii)
103 the CbHap complex(Oda *et al.*, 2015; Oda *et al.*, 2016) (Figure S1b).

104 Although the molecular characteristics of these transcription factors have been
105 studied extensively, details on the molecular mechanism of how methylotrophic yeasts
106 sense methanol concentration and transmit the methanol signal through intracellular
107 signaling pathways to transcription factors are still not very clear. In our previous study,
108 we revealed that Wsc family proteins in *K. phaffii* (KpWsc1 and KpWsc3) play a role in
109 sensing methanol, and that KpWsc1 and KpWsc3 sense a wide range of methanol
110 concentrations and regulate gene expression based on that (Ohsawa *et al.*, 2017). Wsc
111 family proteins are plasma membrane-spanning sensor proteins that have been well
112 characterized in *S. cerevisiae* and are known to activate the cell wall integrity (CWI)
113 pathway in response to cell surface stresses (Levin, 2005). In the CWI pathway, Wsc
114 family proteins interact with ScRom2 and transmit the signal to ScRho1 and the
115 mitogen-activated protein kinase (MAPK) cascade such as ScPkc1, ScBck1,
116 ScMkk1/ScMkk2 and ScMpk1 (Levin, 2005). In *K. phaffii*, there is a clear indication of
117 the involvement of KpRom2 in the methanol signaling pathway (Ohsawa *et al.*, 2017),
118 however, its involvement in the MAPK cascade is not clear.
119 Among the transcription factors involved in the regulation of methanol-induced gene
120 expression in *K. phaffii*, KpMxr1 is the C_2H_2-type transcription factor that is necessary
121 for the activation of many genes, including those involved in peroxisome biogenesis
122 (Lin-Cereghino *et al.*, 2006). In *S. cerevisiae*, the activity of ScAdr1 is regulated
123 through its indirect phosphorylation and dephosphorylation by the ScSnf1/AMPK
124 protein kinase (Ratnakumar *et al.*, 2009). In *K. phaffii*, serine 215 residue of KpMxr1 is
125 phosphorylated under ethanol-culture condition and this phosphoserine interacts with
126 the 14-3-3 protein, resulting in loss of function as a transcription factor (Ohsawa *et al.*,
127 2018; Parua *et al.*, 2012). We have also shown the involvement of S215

phosphorylation of KpMxr1 in ethanol repression of methanol-induced genes (Ohsawa *et al.*, 2018). However, it is still unclear how phosphorylation and dephosphorylation of KpMxr1 affect the CRMI.

In this study, we hypothesized that the transcription factor KpMxr1 is responsible for the CRMI in *K. phaffii* and studied its functional and phosphorylation dynamics. Our results revealed that KpMxr1 receives the methanol signal from Wsc family proteins via KpPkc1 and that this process is independent of the MAPK cascade.

2 RESULTS

2.1 Methanol-induced gene expression and the phosphorylation of KpMxr1 are regulated by the methanol concentration

To identify the transcription factor related to the CRMI, we studied the transcript level of the methanol-induced genes, *AOX1* and *DAS1*, using the transcription factor gene-disrupted strains under various methanol concentrations. As we reported previously, we confirmed that the transcript levels of *AOX1* and *DAS1* in the wild-type strain showed the peak expression with 0.1 % methanol concentration (Figure 1a) (Ohsawa *et al.*, 2017). The transcript level of *KpMXR1* was not affected by methanol concentration (Figure 1a). Cells of *Kpmxr1Δ, Kpmit1Δ, Kptrm1Δ* and *Kphap3Δ* (which is a subunit of KpHap complex) strains grown on glucose media were shifted to YNB medium containing 0.01%, 0.1% or 1% methanol or no methanol (0%) and were incubated for 2 h (Figure 1b). In the *Kptrm1Δ* and *Kphap3Δ* strains, the transcript levels of *AOX1* and *DAS1* peaked with 0.1% methanol and exhibited the pattern similar to the wild-type strain, although the level itself was significantly low (Figure 1b). Notably, the *Kpmxr1Δ* and *Kpmit1Δ* strains completely lost the methanol-induced gene expression seen in the other strains. The expression of *KpMIT1* is induced by methanol and requires transcription factors, KpMxr1, KpTrm1 and a KpHap complex (Figure S1b). Since the transcript level of *KpMIT1* itself exhibited methanol concentration dependence and was found to be under the control of CRMI (Figure 1a), we focused on KpMxr1 for further analyses.

Next, we examined the protein level of KpMxr1 in relation to the methanol concentration. Immunoblot analysis was performed using the strain expressing KpMxr1-FLAG under the control of the *KpMXR1* promoter. Although the protein level

160 of KpMxr1 was remarkably decreased by the medium shift from glucose to methanol,
161 there was no significant difference related to the methanol concentrations tested (Figure
162 1c).
163 Subsequently, we analyzed the phosphorylation state of KpMxr1-FLAG under
164 various methanol concentrations by immunoblot analysis with antibodies against
165 phosphor-serine, phosphor-threonine and phosphor-tyrosine residues. Due to the low
166 expression level of KpMxr1-FLAG protein in methanol culture, the protein was
167 produced under the control of the *ScCUP1* promoter to enable detection in the
168 immunoprecipitated fraction (IP). As shown in Figure S3a, KpMxr1-FLAG was
169 strongly induced by addition of Cu^{2+} into the medium. Cells grown in glucose media
170 containing Cu^{2+} were shifted to YNB media containing 0%, 0.01%, 0.1% or 1%
171 methanol for 30 min, and KpMxr1-FLAG protein was immunoprecipitated with anti-
172 FLAG antibody. When anti-phosphoserine antibody was used, a strong band
173 corresponding to phosphorylated serine was observed under glucose-culture condition,
174 but the band intensity decreased with the medium shift from glucose to methanol,
175 regardless of methanol concentration (Figure 1d). When anti-phosphothreonine
176 antibody was used, we observed a faint phosphorylated threonine band in the glucose-
177 cultured sample, but more intense bands were detected in the methanol-cultured sample
178 with the strongest band at 0.1% methanol (Figure 1d). The phosphorylated tyrosine
179 residue was not detected (Figure 1d). These bands were not detected with the samples
180 from *Kpmxr1Δ* strain (Figure S5d), which confirm the specificity of the antibodies.
181 These results indicate that the total phosphorylation level of serine residues in KpMxr1
182 were higher under glucose-culture condition and lower under methanol-culture
183 condition. In contrast, the threonine residues are phosphorylated under methanol-culture

184 condition in a methanol concentration-dependent manner. These results indicate that the
185 threonine residues in KpMxr1 may play a key role in the control of CRMI.
186
187 **2.2 Identification of the functional region of KpMxr1 responsible for the regulation**
188 **of the CRMI and analysis of phosphorylation state**
189 To survey the possible functional region in KpMxr1 responsible for regulating CRMI,
190 KpMxr1 C-terminal truncated mutant proteins were constructed based on the amino
191 acid sequence alignments of KpMxr1 homologs in methylotrophic yeasts viz. *K. phaffii*
192 Mxr1 (KpMxr1), *C. boidinii* Trm2 (CbTrm2), and *O. polymorpha* Adr1 (OpAdr1)
193 (Figure S2). We speculated that the region crucial for methanol-induced gene
194 expression is well-conserved in the methylotrophic yeasts. Amino acid sequence
195 alignment showed that the DNA binding region and 14-3-3 protein interacting region
196 were conserved in these yeasts, and that 13 other conserved regions were also present in
197 three methylotrophic yeast strains.
198 Next, we designed the C-terminal truncated KpMxr1 proteins, KpMxr1$^{1\text{-}525}$,
199 KpMxr1$^{1\text{-}368}$, KpMxr1$^{1\text{-}230}$ and KpMxr1$^{1\text{-}211}$ (Figure 2a). These KpMxr1-truncated
200 mutant proteins tagged with FLAG were expressed in the *Kpmxr1Δ* strain under the
201 *KpMXR1* promoter (Figure S3b) and the resulting strains were named TM525, TM368,
202 TM230 and TM211, respectively. A previous report showed that the 1-400 a.a. region
203 of KpMxr1 is sufficient for its function in methanol-induced gene expression (Parua *et*
204 *al.*, 2012). The *AOX1* transcript level of the control strain FL1155 expressing full length
205 KpMxr1 (KpMxr1^{FL})-FLAG and the TM525 strain showed a similar pattern (Figure
206 2b). However, the transcript level of the TM368 strain decreased in 0.1% and 1% of
207 methanol compared to the control strain, and that of the TM230 strain decreased in all

methanol concentrations (Figures 2b and S4a). Interestingly, the *AOX1* transcript level in the TM211 strain under 0.1% and 1% conditions was higher than that in the TM230 strain (Figure 2b), which supports the assumption that the region from 212 to 230 a.a., which includes the interaction site with 14-3-3 protein, plays a role in repressing the *AOX1* gene expression under high (> 0.1%) methanol conditions.

Regarding the effect of KpMxr1 truncation on growth on methanol, a previous study reported that the strain expressing KpMxr1$^{1\text{-}400}$ under the control of the glyceraldehyde-3-phosphate dehydrogenase (*GAP*) gene promoter was incapable of growth on 1% methanol medium (Gupta *et al.*, 2021). In this study, we used the original *KpMXR1* promoter, and the strains TM525 and TM368 exhibited similar growth as the control strain FL1155 (Figure 2c). Overexpressed truncated KpMxr1$^{1\text{-}400}$ expressed by the strong *GAP* promoter may cause growth defect on methanol. We observed a significant growth delay in strains TM230 and TM211 (Figure 2c). From these results, it is clear that the region from 230 to 368 has an indispensable function in cell growth on methanol. Growth on glucose and ethanol was not affected by KpMxr1 truncation except that the TM211 strain exhibited a slight growth defect on ethanol (Figures S4b and S4c).

KpMxr1 has been reported to be distributed in the cytosol under glucose-culture condition and localized to the nucleus by the medium shift from glucose to methanol (Lin-Cereghino *et al.*, 2006). Truncated KpMxr1$^{1\text{-}400}$ has been shown to be localized to the nucleus under both glucose- and methanol-culture conditions (Gupta *et al.*, 2021). While KpMxr1^{FL}-YFP localized to the nucleus in all concentrations of methanol, there was no difference in KpMxr1^{FL}-YFP localization based on the methanol concentrations in the medium (Figure S4d). Truncated KpMxr1$^{1\text{-}525}$-YFP and KpMxr1$^{1\text{-}230}$-YFP

localized in the nucleus under glucose- or methanol-culture conditions (Figure S4e). These results suggested that the truncated KpMxr1 proteins contain the nuclear localization signal (NLS) but lacked a nuclear export signal (NES) and the decrease in *AOX1* transcript level in strains possessing truncated KpMxr1 proteins (Figure 2b) is not a result of the deficiency in nuclear localization.

KpMxr1 protein has a large molecular mass (1155 amino acids, 141.4 kDa) and it is expected to have multiple phosphorylation sites. Indeed, KpMxr1-FLAG protein was detected in gels with or without phos-tag, but the phosphorylated KpMxr1 bands were unclear and their differences could not be evaluated. To improve the resolution of the phosphorylation state of KpMxr1 by phos-tag SDS-PAGE, strains expressing truncated KpMxr1 mutants were used in the following analyses instead of the full-length strain.

As shown in Figures 2d and S3c, the intensity of the phosphorylated bands decreased due to the medium shift from glucose to methanol in strains TM525, TM368 and TM230. In the TM230 strain, at least 6 phosphorylated bands were detected in glucose-cultured cells and some upper bands were not detected in methanol-cultured cells (Figure 2d). These results suggest that KpMxr1 has multiple phosphorylation sites, and some of them are dephosphorylated by the medium shift from glucose to methanol.

Subsequently, the phosphorylation state of KpMxr1$^{1\text{-}230}$ under various methanol concentrations was analyzed. FLAG-tagged KpMxr1$^{1\text{-}230}$ was immunoprecipitated and subjected to phos-tag SDS-PAGE analysis (Figures 2e and S3d). KpMxr1$^{1\text{-}230}$ was highly phosphorylated in 1% methanol-cultured cells, and it was comparable to the level of glucose-cultured cells. This indicates that highly phosphorylated KpMxr1 is involved in repression of *AOX1* gene expression at 1% methanol condition.

256 **2.3 Analysis of multiple phosphorylated residues in KpMxr1**

257 LC-MS/MS analysis of FLAG-tagged KpMxr1$^{1-525}$ was performed to survey the
258 phosphorylation sites in KpMxr1 under glucose- or methanol-culture conditions.
259 Samples were purified by immunoprecipitation, confirmed by western blot analysis and
260 using a CBB-stained gel. Phosphorylated sites of KpMxr1$^{1-525}$ under glucose- and
261 methanol-culture conditions are summarized in Figure 3a. Amino acid residues S110
262 and S111 were significantly phosphorylated both in the glucose-cultured and methanol-
263 cultured samples and the phosphorylation levels were higher in the glucose-cultured
264 sample. Similar phosphorylation states were observed for other serine residues, e.g.,
265 S116, S149, S190, S215 and S217. On the other hand, the phosphorylation level of
266 T121, T124, T125 T128 and T131 were higher in the methanol-cultured samples. These
267 results show that KpMxr1 harbor multiple phosphorylation sites in addition to S215 that
268 was reported previously (Parua *et al.*, 2012), and indicate that these threonine- and
269 serine-residues were phosphoregulated in accordance with the medium shift from
270 glucose to methanol.

271 A previous study reported that S215 in KpMxr1 is phosphorylated on ethanol culture
272 and this phosphorylation is crucial for its interaction with 14-3-3 protein (Parua *et al.*,
273 2012). We demonstrated that the phosphorylation of S215 is responsible for ethanol
274 repression of methanol-induced genes (Ohsawa *et al.*, 2018). But in this study, we found
275 that the S215A mutation of KpMxr1 did not affect the peak pattern of the CRMI (Figure
276 S5a). We also found that there was no difference in the cell growth on methanol
277 between the strains expressing KpMxr1-FLAG and KpMxr1(S215A)-FLAG (Figure
278 S5b).

279 Based on the results from LC-MS/MS, we constructed strains containing mutations in
280 putative phosphorylation sites of KpMxr1, i.e., KpMxr1$^{T121A, T124A, T125A, T128A, T131A}$ (TA
281 mutant) and KpMxr1$^{S110A, S111A}$ (SA mutant). CRMI was analyzed with strains
282 expressing KpMxr1^{FL}-TA-FLAG and KpMxr1^{FL}-SA-FLAG (MTA and MSA) under the
283 control of the *KpMXR1* promoter in order to evaluate the effect of TA and SA mutations
284 on the CRMI. The *AOX1* transcript level was determined at various methanol
285 concentrations with strains MTA and MSA compared with the control strain expressing
286 KpMxr1^{FL}-FLAG (Figure 3b). The TA mutant strain MTA showed decrease in the
287 *AOX1* transcript level at 0% and 0.01% methanol-culture conditions. Moreover, the
288 peak of *AOX1* transcript level in strain MTA was detected at 0.1% methanol, while the
289 peak of the control strain was at 0.03%. Therefore, the expression peak of *AOX1* shifted
290 to a higher methanol concentration in strain MTA, which seemed to be due to an
291 impairment in methanol-sensing at low methanol concentrations (less than 0.03%).
292 Considering that phosphoregulation of threonine residues depends on methanol
293 concentration (Figure 1d), these results indicate that phosphorylation of threonine
294 residues of KpMxr1 (T121/T124/T125/T128/T131) plays a critical role in CRMI. On
295 the other hand, the SA mutant strain MSA showed decrease in the *AOX1* transcript level
296 at low methanol concentrations (0% and 0.01%) and increase in the expression level at
297 1% methanol. Although the peak of the *AOX1* expression did not change in strain MSA,
298 phosphorylation of serine residues (S110/S111) may also be involved in CRMI at lower
299 methanol concentration.
300 We investigated the effect of SA and TA mutations on the phosphorylation state of
301 KpMxr1 using the TM230SA and TM230TA strains (Figures 3c and S5c). Consistent
302 with the result of Figures 2d and 2e, the strain expressing KpMxr1$^{1-230}$-FLAG exhibited

303 multiple bands and the intensity of the phosphorylated bands decreased by medium shift
304 from glucose to methanol (Figure 3c). The band indicated by the black arrowhead
305 observed in the sample from the glucose-grown cells expressing KpMxr1$^{1\text{-}230}$-FLAG
306 was not detected in the sample from the TM230SA strain (Figure 3c). Moreover, this
307 band was lost in the samples from all strains under methanol-culture condition (Figure
308 3c). From these results, the residues S110 and/or S111 in KpMxr1 are suggested to be
309 phosphoregulated during CRMI. The phosphorylation of threonine and serine residues
310 of KpMxr1 in MTA and MSA strains was analyzed using anti-phosphothreonine and
311 anti-phosphoserine antibodies (Figure S5d). In the immunoprecipitated samples of all
312 strains, threonine residues were phosphorylated by the medium shift from glucose to
313 methanol, and serine residues were dephosphorylated in total by the medium shift. This
314 result was consistent with the phosphorylation level of threonine and serine residues
315 (Figure 1d). The phosphorylated bands were not lost by TA and SA mutations,
316 suggesting that KpMxr1 has phosphorylation sites other than the mutated threonine and
317 serine residues (T121/T124/T125/T128/T131 and S110/ S111). The effect of TA and
318 SA mutations in KpMxr1 for the growth on methanol was also investigated (Figure
319 S5e). There were no obvious differences in the growth on 0.1, 0.5 or 1% methanol
320 among the control, MTA and MSA strains.
321
322 **2.4 KpMxr1 receives the methanol signal from KpPkc1 but not from the MAPK**
323 **cascade**
324 We then focused on the signal transduction pathway with respect to CRMI. Previously,
325 we reported that KpWsc1 and KpWsc3 contribute toward sensing the environmental
326 methanol concentration and that KpWsc1 responds to a lower range of methanol

concentrations than KpWsc3 (Ohsawa *et al.*, 2017). In *S. cerevisiae*, Wsc family proteins are known to be a cell surface stress sensor that transmits the signal to the CWI pathway through the MAPK cascade (Levin, 2005). The downstream regulators of Wsc family proteins are GTP-binding protein ScRho1, protein kinase C (ScPkc1) and MAPKK protein (ScMkk1), and their dominant active mutants ScRho1^{Q68H} (GTP-locked mutant), ScPkc1^{R398P} and ScMkk1^{S386P} are known (Madaule *et al.*, 1987; Nonaka *et al.*, 1995; Yashar *et al.*, 1995). To investigate the involvement of downstream regulators of KpWsc1 and KpWsc3 in the CRMI, *K. phaffii* strains corresponding to each hyperactive mutant, i.e., KpRho1^{Q68H}, KpPkc1^{R390P} and KpMkk1^{S313P}, together with their wild type proteins, were constructed under the *ScCUP1* promoter. We confirmed that the levels of expressed proteins increased with the added Cu^{2+} concentration to the medium, and we also confirmed the activation of MAPK cascade using immunoblot analysis with anti-phospho-Mpk1 antibody in the hyperactive mutant proteins, but not in control proteins (Figure 4a-c upper panels).

The transcript level of *AOX1* decreased with the induction of hyperactive mutant proteins KpRho1^{Q68H} (Figures 4a lower panel) and KpPkc1^{R390P} (Figures 4b lower panel). On the other hand, expression of KpMkk1^{S313P} did not affect the *AOX1* transcript level (Figures 4c lower panel). These results indicate that the methanol signal from Wsc family proteins is transmitted to KpRho1 and then to KpPkc1, but not to KpMkk1, indicating that the CRMI pathway is not downstream of the MAPK cascade.

In order to discern which transcription factor receives the methanol signal, the *AOX1* transcript levels in the transcription factor-deleted *K. phaffii* strains, i.e., *Kpmxr1*Δ*, Kpmit1*Δ*, Kptrm1*Δ*, Kphap3*Δ*, Kpmig1*Δ *and Kprop1*Δ, were investigated under the expression of KpRho1^{Q68H}. As shown in Figure 4d, the *AOX1* transcript level in the

Kpmxr1Δ strain was not affected by the induction of KpRho1^{Q68H}, but it was reduced in all the other strains. These results imply that KpMxr1 receives the methanol signal from Wsc family proteins via KpRho1.

To understand how the activated signal transduction affects the phosphorylation state of KpMxr1, hyperactive KpPkc1^{R390P}-HA was expressed under the control of the *ScCUP1* promoter. The protein level of hyperactive KpPkc1^{R390P}-HA was confirmed to be induced by the addition of 50 μM Cu^{2+} to the SM medium (Figure 5a left panel). The amount of KpMxr1$^{1-230}$-FLAG slightly decreased by inducing KpPkc1^{R390P} under methanol-culture conditions (Figure 5a left panel).

Our earlier observation showed that the phosphorylation level of KpMxr1$^{1-230}$-FLAG was reduced with the medium shift from glucose to methanol (Figure 2d). But we observed that the phosphorylation level increased with the expression of hyperactive KpPkc1^{R390P}-HA and the addition of 50 μM Cu^{2+} in the medium after the medium shift to methanol medium for 30 min (Figure 5a right panel). Both the protein level of KpPkc1^{R390P}-HA and the phosphorylation level of KpMpk1 increased with increase in Cu^{2+} concentration (Figure 5b). The protein level of KpMxr1-FLAG decreased with the increase of Cu^{2+} concentration (Figure 5b), while there were no significant differences in the KpMxr1 protein level related to the methanol concentration (Figure 1c). Next, we examined the *AOX1* transcript level after the medium shift for 30 min with the addition of various concentrations of Cu^{2+}. The *AOX1* transcript level showed the peak pattern (maximum. at 1 μM) with the increase of KpPkc1^{R390P}-HA protein, which was similar to the response observed for the increase in methanol concentration (Figure 5c). These results imply that KpPkc1 receives the methanol signal, which then leads to the CRMI. The phosphorylation level of KpMxr1$^{1-230}$-FLAG according to the induction level of

375 KpPkc1^{R390P}-HA by increasing Cu^{2+} concentration was also observed under 0.1%
376 methanol-culture condition (Figure S6). From these results, we concluded that KpMxr1
377 receives the methanol signal from Wsc family proteins via KpPkc1 in the regulation of
378 the CRMI.
379

3. DISCUSSION

In nature and in the fermenter, methylotrophic yeasts sense environmental methanol concentration and regulate the expression level of their methanol-induced genes to avoid unbalanced methanol metabolism that may result in the accumulation of formaldehyde, a toxic metabolite. In addition to the transcription factors involved in methanol-induced gene expression, we previously reported that the Wsc family proteins are involved in methanol sensing (Ohsawa *et al.*, 2017; Yurimoto *et al.*, 2019). However, it is unclear how methylotrophic yeasts transmit the methanol signal to transcription factors. Results of the present study revealed that KpMxr1 is involved in regulation of the CRMI and that its phosphorylation is regulated through the novel methanol signaling pathway from Wsc family proteins via KpPkc1 to KpMxr1 (CRMI pathway), which is independent of the MAPK cascade (Figure 6).

The phosphorylation state of KpMxr1 is dependent on the carbon sources and methanol concentration (Figures 1d, 2d and 2e). The serine residues in KpMxr1 were highly phosphorylated under glucose-culture condition and partly dephosphorylated under methanol-culture condition (Figure 1d). On the other hand, the threonine residues were phosphorylated in the methanol culture in a concentration-dependent manner with a peak at 0.1% methanol concentration (Figure 1d); this pattern correlated with the regulatory profile of methanol-induced gene expression (Figure 1a). The total phosphorylation level of KpMxr1$^{1\text{-}230}$-FLAG was decreased by the medium shift from glucose to methanol medium (Figures 2d and 2e) and changed depending on the methanol concentration (Figure 2e).

403 Our results from truncated KpMxr1 mutant analyses (Figures 2b and 2c) suggest that
404 the 231-368 a.a. region of KpMxr1 is responsible for response to lower methanol
405 concentrations (0.01-0.1%) and the 369-525 a.a. region for response to higher methanol
406 concentration (0.1-1.0%). These regions contained conserved regions 1-5 in KpMxr1
407 homologs in methylotrophic yeasts (Figure S2) indicating the conserved function of
408 KpMxr1 in the CRMI among the methylotrophic yeasts. Interestingly, the *AOX1*
409 transcript level increase in TM211 with increasing methanol concentration (0.1 to 1.0%)
410 (Figure 2b). The amino acid region from 212 to 230 containing three serine residues
411 S215/S217/S220 may be involved in CRMI through phosphoregulation.
412 The regulation of KpMxr1 subcellular localization is also an interesting issue. The
413 $KpMxr1^{FL}$-YFP was distributed in the cytosol under glucose-culture condition and
414 localized to the nucleus under methanol-culture condition (Figure S4d). However,
415 truncated KpMxr1 proteins remained in the nucleus under both glucose- and methanol-
416 culture conditions (Figure S4e), which may be due to the lack of NES region. Further
417 analyses will be needed to elucidate where KpMxr1 is phosphor regulated and how its
418 subcellular localization is affected by phosphoregulation.
419 In *S. cerevisiae*, ScAdr1, a homolog of KpMxr1, has been reported as a transcription
420 factor that activates genes involved in the utilization of nonfermentable carbon sources
421 (Young *et al.*, 2003), and that its activity is controlled by the AMP-activated protein
422 kinase ScSnf1 via the dephosphorylation of the serine residue S230 (Ratnakumar *et al.*,
423 2009). The serine residue S215 in KpMxr1, which corresponds to S230 in ScAdr1, has
424 been reported to be phosphorylated under glucose- or ethanol-culture conditions, and
425 that the phosphorylated S215 interacts with 14-3-3 protein to inactivate KpMxr1 (Parua
426 *et al.*, 2012). In this study, LC-MS/MS analysis revealed that multiple serine and

427 threonine residues in KpMxr1 are phosphorylated (Figure 3a). Mutation of some of
428 these residues resulted in decrease in the *AOX1* transcript level under lower methanol
429 concentration conditions (< 0.03%) (Figure 3b). On the other hand, SA and TA
430 mutations of KpMxr1 did not influence the growth on methanol medium (Figure S5e).
431 As S215A mutation did not influence the growth on methanol (Figure S5b), non-
432 phosphorylatable mutation of serine or threonine residues may not be sufficient to cause
433 a deficiency in the cell growth.
434 In *K. phaffii*, methanol-sensing Wsc family proteins play a role not only in regulating
435 methanol-induced gene expression, but also in negatively regulating pexophagy, the
436 degradation process of peroxisomes (Ohsawa *et al.*, 2021). In the presence of methanol
437 (0.15-2%), KpWsc1 transmits the methanol signal via the MAPK cascade (KpMpk1) to
438 the transcription factor Rlm1, which activates expression of phosphatase genes related
439 to phosphoregulation of KpAtg30. The CRMI pathway we demonstrate here does not
440 involve the MAPK cascade and the methanol signal is transmitted to KpMxr1 through
441 the pathway that is branched out from KpPkc1 (Figures 4, 5 and 6). In the strains
442 overexpressing hyperactive mutants KpRho1^{Q68H} or KpPkc1^{R390P}, the *AOX1* transcript
443 level decreased (Figures 4a and 4b), which may be caused by the strong methanol
444 signal. In other words, overexpression of KpRho1^{Q68H} or KpPkc1^{R390P} mimics the
445 condition of high methanol concentration.
446 In general, gene expression is regulated simply in an on/off manner, and the strength
447 of the expression is usually dependent on the dose of the inducer and the expression
448 level eventually reaches a plateau. However, in CRMI, methanol-induced gene
449 expression essentially needs to be regulated more delicately to avoid unbalanced
450 methanol metabolism resulting in the accumulation of formaldehyde. In order to achieve

such a "delicate" regulation, *K. phaffii* seems to have developed a sophisticated mechanism as follows: after Wsc family proteins sense the environmental methanol concentration, the methanol signal is transmitted to KpRom2, KpRho1, and then to KpPkc1. The KpPkc1 activity determined by the methanol-signal strength presumably determines the signal strength to the CRMI pathway regulating the phosphorylation state of KpMxr1. Various phosphorylation patterns of KpMxr1 at multiple phosphorylation sites then determine the molecular structure of KpMxr1 depending on the methanol signal, which regulates the level of downstream methanol-induced gene expression (Figure 6).

In the future, we want to identify the kinase or phosphatase that directly reacts with KpMxr1. Based on the screening analysis of the kinases in *K. phaffii*, 152 annotated kinases involved in cell growth and *AOX1* promoter regulation were identified, and they include one of the three β-subunits of the KpSnf1 complex, KpGal83 (Shen *et al.*, 2016). In *S. cerevisiae*, Snf1 complex controls the activity of ScAdr1, but Snf1 complex is not a direct kinase of ScAdr1. Therefore, there must be other yet unknown kinases and phosphatases downstream of KpPkc1 or KpSnf1 complex. Further research in this area would help unravel these downstream players and their specific roles in methanol-induced gene expression in *K. phaffii*.

4. MATERIALS AND METHODS

4.1 Strains and media

Escherichia coli HST08 Premium (Takara Bio, Otsu, Japan) was used as a host strain for plasmid DNA preparation. *E. coli* cells were grown in LB medium (1% tryptone, 0.5% yeast extract, 0.5% NaCl) at 37 ˚C.

The yeast strains used in this study are listed in Table S1. *K. phaffii* cells were grown on YPD (1% yeast extract, 2% peptone, 2% glucose) or YNB medium (0.67% yeast nitrogen base without amino acids, pH 6.0). 2% (w/v) glucose (synthetic dextrose medium; SD medium), 0.5% (v/v) ethanol (SE medium) or several concentrations of methanol (SM medium) were used as carbon sources in YNB medium. All the components other than the carbon sources used in these media were purchased from Difco Becton Dickinson (Franklin Lakes, NJ). The growth of the yeast was monitored by the optical density (OD) at 610 nm.

4.2 Plasmid construction and gene disruption

The plasmids used in this study are listed in Table S2. The oligonucleotide primers in this study are listed in Table S3. A gene deletion cassette for *KpTRM1* was constructed as follows: Primer pairs GeneD-trm1-A-Fw/GeneD-trm1-A-Rv and GeneD-trm1-B-Fw/GeneD-trm1-B-Rv were used to amplify 1.0 kbp of DNA from the genome (namely fragment A, B). The primer pair (trm1)-Bsd-Fw/(trm1)-Bsd-Rv was used to amplify the blasticidin S resistance gene using plasmid pPIC6A (Thermo Fisher Scientific, Waltham, MA) as template (fragment C). These three fragments were combined by overlap PCR with the primer pair GeneD-trm1-A-Fw/GeneD-trm1-B-Rv, and a 3.1-kbp fragment (A-C-B) was obtained. This fragment was cloned (TA cloning) into the TOPO

494 vector pCR2.1 (Takara Bio, Otsu, Japan), yielding the *KpTRM1* disruption vector
495 pKI001. pKI001 was digested with EcoRI to disrupt the *KpTRM1* gene. These digested
496 DNA fragments were used to transform *K. phaffii* by electroporation. Proper gene
497 disruptions were confirmed by colony PCR. Gene deletion of *KpHAP3*, *KpMIT1,*
498 *KpMIG1* or *KpROP1* was performed by the same way using the primer pairs listed in
499 Table S3.
500 For copper-inducible expression of *KpMXR1*, the region from -235 to -1 of the
501 *ScCUP1* promoter was amplified by PCR from *S. cerevisiae* genomic DNA as template
502 using the primer pair Infusion-Pcup1-pIB1arg-Fw/Infusion-Pcup1-pIB1arg-Rv. This
503 fragment was cloned into the KpnI and BamHI sites of pSN303 by In-Fusion cloning
504 (Takara Bio, Otsu, Japan), resulting in pKI006.
505 The *KpMXR1* promoter and the DNA region of KpMxr1 1-525 a.a., 1-368 a.a., 1-230
506 a.a. and 1-211a.a. were amplified by PCR using primer pairs Inverse-Mxr1-5xFLAG-
507 Fw/ Infusion-Mxr1(525)-Rv, Infusion-Mxr1-5xFLAG-Fw/Infusion-Mxr1(368)-Rv,
508 Inverse-Mxr1-5xFLAG-Fw/Infusion-Mxr1(230)-Rv and Inverse-Mxr1-5xFLAG-
509 Fw/Infusion-Mxr1(211)-Rv for pKI007, pKI008, pKI009 and pKI010, respectively.
510 They were cloned into the KpnI and BamHI sites of pSN303 by In-Fusion cloning.
511 The *KpMXR1* promoter and the DNA region of KpMxr1 1-1155 a.a., 1-525 a.a. and
512 1-230 a.a. were amplified by PCR using primer pairs Infusion-Pmxr1-Mxr1-
513 Fw/Infusion-Mxr1YFP-Rv, Infusion-Pmxr1-Mxr1-Fw/Infusion-Mxr1(525)YFP-Rv and
514 Inverse-Mxr1-5xFLAG-Fw/Infusion-Mxr1(230)-Rv for pKI011, pKI012 and pKI013
515 respectively. They were cloned into the KpnI and BamHI sites of pNT205 by In-Fusion
516 cloning.

pSN303 was subjected to site-directed mutagenesis by using the primer pairs Mutation-Mxr1-S(2)A-Fw/Mutation-Mxr1-S(2)A-Rv and Mutation-Mxr1-T(5)A-Fw/Mutation-Mxr1-T(5)A-Rv, resulting in pKI014 and pKI015, respectively. The *KpMXR1* promoter and the DNA region of KpMxr1 1-230 a.a. were amplified by PCR from pKI014 and pKI015 using primer pair Inverse-Mxr1-5xFLAG-Fw/Infusion-Mxr1(230)-Rv, resulting in pKI016 and pKI017, respectively.

The region from -235 to -1 of the *ScCUP1* promoter was amplified by PCR from *S. cerevisiae* genomic DNA as template using the primer pair EcoRI-CUP1promoter-Fw/EcoRI-CUP1promoter-Rv. The DNA fragment and pIB1 were digested by EcoRI and ligated to obtain the plasmid Pc(EcoRI)-pIB1. The gene *KpRHO1* N-terminal tagged with myc was amplified by PCR from *K. phaffii* genomic DNA as template using the primer pair KpnI-Myc-Rho1-Fw/HindIII-Rho1-Rv. The DNA fragment and Pc(EcoRI)-pIB1 were digested by HindIII and KpnI and ligated to obtain pKI018. The region from -235 to -1 of the *ScCUP1* promoter was amplified by PCR from *S. cerevisiae* genomic DNA as template using the primer pair KpnI-CUP1promoter-Fw/KpnI-CUP1promoter-Rv. The DNA fragment and pSY006 were digested by KpnI and ligated to obtain the plasmid Pc(KpnI)-pSY006. The gene *KpPKC1* and *KpMkk1* was amplified by PCR from *K. phaffii* genomic DNA as template using the primer pairs BamHI-Pkc1-Fw/ Xho1-Pkc1-Rv and XmaI-Mkk1-Fw/PstI-Mkk1-Rv, respectively. The DNA fragments and Pc(KpnI)-pSY006 were digested by BamHI/XhoI and XmaI/PstI, and then ligated to obtain pKI019 and pKI020, respectively. pKI018, pK019 and pKI020 were subjected to site-directed mutagenesis by using the primer pairs Rho1-Q68H-Fw/Rho1-Q68H-Rv, Pkc1-R390P-Fw/Pkc1-R390P-Rv and Mkk1-S313P-Fw/Mkk1-S313P-Rv, resulting in pKI021, pKI022 and pKI023, respectively.

541

542 **4.3 RNA isolation and quantitative reverse transcription (qRT-PCR)**

543 A single colony was inoculated in YPD medium and grown overnight at 28°C. Yeast
544 cells were transferred into SD medium and cultivated to early exponential phase. The
545 cells were shifted to SM medium and cultured for 2 h. Cells equivalent to 5 OD_{610} units
546 were harvested at the indicated time point by centrifugation at 10,000 g for 1 min at 4
547 ˚C. Total RNA was extracted from cells and RT-PCR was performed following the
548 procedure described in (Ohsawa *et al.*, 2018). The PCR primers for *AOX1, DAS1,*
549 *MXR1, MIT1* and *GAP* are listed in Table S3.

550

551 **4.4 Preparation of protein extracts from yeast cells**

552 Yeast cells were grown in YPD and SD as described above, and the cells were shifted
553 from SD to SM medium at 28 ˚C for 30 min to 2 h. The cells equivalent to about 2
554 OD_{610} units (for immunoblot analysis), 100 OD_{610} units (for immunoprecipitation and
555 immunoblot analysis) or 2,000 OD units (for immunoprecipitation and LC-MS/MS
556 analysis) were cultured and collected for protein extraction. They were suspended in 0.2
557 N NaOH solution containing 0.5% β-mercaptoethanol for 15 min on ice and
558 trichloroacetic acid was added to a final concentration of 10% v/v for cell lysis. The
559 samples were centrifuged (20,000 g, 5 min, 4 °C) and protein pellets were washed three
560 times by 100% acetone by a brief sonication. Subsequently, protein pellets were re-
561 suspended in the sample buffer (62.5 mM Tris-HCl, 2% SDS, 10% Glycerol, 5% β-
562 mercaptoethanol, 0.005% BPB, pH 6.8) or the buffer for immunoprecipitation (62.5
563 mM Tris-HCl, 2% SDS, pH 6.8). The samples were incubated at 65°C for 10 min.

564

565 **4.5 Immunoprecipitation**

566 To the obtained protein extract solution, 20 times the amount of the buffer without SDS
567 (62.5 mM Tris-HCl, protease inhibitor cocktail (Roche Diagnostics, Basel,
568 Switzerland), and phosphatase inhibitor cocktail (Nakalai tesque, Kyoto, Japan), pH
569 6.8) were added. The solution was pre-cleared with mouse IgG-Agarose beads (Merck
570 KGaA, Darmstadt, Germany) for 2 h at 4 °C to remove nonspecific binding proteins.
571 Mouse IgG-agarose beads and protein debris were removed by centrifugation in a swing
572 rotor at 1,500 g for 10 min. Anti-FLAG-M2 affinity agarose beads (Merck KGaA,
573 Darmstadt, Germany) were added and incubated for 2 h at 4 °C. The beads were
574 collected by centrifugation in a swing rotor at 1,500 g for 5 min and washed by 62.5
575 mM Tris-HCl buffer (pH 6.8). For LC-MS/MS analysis, the target protein was eluted
576 with the sample buffer for 20 min at 80 °C, and the eluted protein sample was
577 condensed by ultra-filtration with amicon ultra-4 centrifugal filter 50K (Merck KGaA,
578 Darmstadt, Germany). For phos-tag SDS-PAGE, anti-FLAG-M2 affinity agarose beads
579 harboring the target protein were washed and treated with or without λ-phosphatase
580 (New England Biolabs, Ipswich, MA, USA) at 30 ℃ for 1 h. Then, the target protein
581 was eluted with the sample buffer for 20 min at 80 °C.

582

583 **4.6 Immunoblot analysis**

584 The samples were first centrifuged at 20,000 × g for 1 min. 10 μL of the supernatant
585 was electrophoresed on a 6-10% SDS-PAGE gel. Precision Plus Protein Dual Color
586 Standard (Bio-Rad, Hercules, USA) was used as a protein-loading marker. The proteins
587 were transferred to a Immobilon-P PVDF membrane (0.2 μm, Merck KGaA, Darmstadt,
588 Germany) by semidry blotting (Bio-Rad, Hercules, USA). The membranes were

589 incubated in Blocking One (Nakalai tesque, Kyoto, Japan) and then in anti-
590 DYKDDDDK antibody (called anti-FLAG antibody in this study, 1E6; Fujifilm, Tokyo,
591 Japan), anti-beta actin (Abcam, Cambridge, UK), anti-phosphoserine antibody (Abcam,
592 Cambridge, UK), anti-phosphothreonine antibody (Abcam, Cambridge, UK) or anti-
593 phosphotyrosine antibody (Abcam, Cambridge, UK) at dilutions recommended in the
594 protocol with TBS-T buffer. The membranes were washed 3 times with TBS-T buffer
595 and incubated with anti-mouse-HRP (Merck Millipore, Darmstadt, Germany) or anti-
596 rabbit-HRP at a 1:5,000 dilution for 1 h. Finally, bound secondary antibodies were
597 detected using Western Lightning (Perkin-Elmer Life Science, Waltham, MA) and the
598 signals were detected using Lummino-Graph II (ATTO, Tokyo, Japan). The band
599 intensity was quantified with ImageJ (National Institutes of Health, USA).
600 In the phos-tag analysis, SuperSep gels with or without 50 μM phos-tag (7.5%,
601 13wells; Fujifilm, Tokyo, Japan) were mainly used. Hand-made gels containing Zn^{2+}
602 were also used with or without 20 μM of phos-tag (8.5% Wako, Osaka, Japan)
603 according to the instruction manual of Wako.
604
605 **4.7 LC-MS/MS analysis**
606 The protein samples purified by immunoprecipitation were loaded in 12.5% SDS-PAGE
607 gels. The electrophoresed gels were stained with CBB Stain One Super (Nakalai tesque,
608 Kyoto, Japan), and a part of the gel of the target protein band was cut out. The gels were
609 digested using an in-gel tryptic digestion kit (Thermo Fisher Scientific) according to the
610 manufacturer's instruction. The recovered tryptic digests were separated using nano-
611 flow liquid chromatography (Nano-LC-Ultra 2D-plus equipped with cHiPLC Nanoflex,
612 Eksigent, Dublin, CA, USA) in a trap and elute mode, with a trap column (200 μm x 0.5

613 mm ChromXP C18-CL 3 μm 120 Å (Eksigent)) and an analytical column (75 μm x 15
614 cm ChromXP C18-CL 3 μm 120 Å (Eksigent)). The gradient program used for the
615 separation was as follows; A98%/B2% to A66.8%/B33.2% in 125 min,
616 A66.8%/B33.2% to A2%/B98% in 2 min, A2%/B98% for 5 min, A2%/B98% to
617 A98%/B2% in 0.1 min, and A98%/B2% for 17.9 min, in which 0.1% formic acid/water
618 and 0.1% formic acid/acetonitrile were utilized as mobile phases A and B, respectively.
619 The flow rate was 300 nL/min. The analytical column temperature was 40 ºC. The
620 eluate was directly infused into a mass spectrometer (TripleTOF 5600+ System coupled
621 with a NanoSpray III source and heated interface, SCIEX, Framingham, MA, USA),
622 and ionized in the electrospray ionization-positive mode. Data acquisition was
623 performed using an information-dependent acquisition method. The acquired datasets
624 were analyzed using ProteinPilot software, version 5.0.1 (SCIEX), with the NCBI
625 protein library for *K. phaffii* (April 2020) appended with the amino acid sequence of
626 KpMxr1$^{1\text{-}525}$-FLAG and known contaminants database (SCIEX). Various protein
627 modifications were detected in KpMxr1, such as phosphorylation, oxidation,
628 methylation, acetylation etc., Identifications with at least 95% confidence were
629 considered significant.
630

631 **4.8 Fluorescence microscopy observation**

632 Yeast cells were grown in YPD and SD as described above, and the cells were shifted
633 from SD to SM medium containing 0, 0.01, 0.1 or 1 % methanol at 28 ˚C for 3 h. The
634 cells were treated with 5% formaldehyde (using 35% formaldehyde solution containing
635 7% methanol, Nakarai chemicals, Japan) for 1h, and subsequently incubated in DAPI
636 solution (100 μg/L, Nacalai tesque, Kyoto , Japan) for 30 min. Observations were

carried out with an IX81 fluorescence microscope (Olympus, Tokyo, Japan). Fluorescent images were captured with a charged coupled device (CCD) camera (SenSys; PhotoMetrics, Tucson, AZ) using MetaMorph software (Universal Imaging, West Chester, PA).

4.9 Statistical analysis

All data were obtained from three independent biological replicates and presented as mean ± S.E. Student's t test was performed to determine the differences among grouped data. Statistical significance was assessed at $p < 0.05$. For comparison between some groups, parametric one way analysis of variance based on Turkey- Kramer test was performed.

AUTHOR CONTRIBUTIONS

KI, SO, HY and YS designed the experiments and KI and SO performed them. SI performed the LC-MS/MS analysis. KI, SO, SI, HY and YS were involved in the discussion of results and writing of the manuscript.

ACKNOWLEDGEMENTS

This research was supported in part by Grant-in-Aid for Scientific Research on Innovative Areas (19H05709 to YS), Grant-in-Aid for Scientific Research (B) (19H04326 and 22H03802 to HY) and Grant-in-Aid for JSPS Fellows (19J21821 to KI) from the Japan Society for the Promotion of Science. This research was also supported in part by grants from the Institution of Fermentation, Osaka (IFO) and Noda Institute of Scientific Research to HY.

CONFLICT OF INTEREST

The authors declare no conflicts of interest.

ETHICS STATEMENT

This research did not use human or animal subjects. The recombinant DNA experiments were performed according to the guidelines by Environment, Safety and Health Committee of Kyoto University.

DATA AVAILABILITY STATEMENT

The data that support the findings of this study are available in the supplementary material of this article.

SUPPORTING INFOMATION

Additional supporting information may be found in the online version of the article at the publisher’s website.

678 **REFERENCES**

679 Cregg, J.M., Lin-Cereghino, J., Shi, J., and Higgins, D.R. (2000) Recombinant protein
680 expression in *Pichia pastoris*. *Molecular Biotechnology* **16**: 23–52.
681 https://doi.org/10.1385/MB:16:1:23

682 De, S., Mattanovich, D., Ferrer, P., and Gasser, B. (2021) Established tools and
683 emerging trends for the production of recombinant proteins and metabolites in *Pichia*
684 *pastoris*. *Essays in Biochemistry* **65**: 293–307. https://doi.org/10.1042/EBC20200138

685 Gellissen, G. (2000) Heterologous protein production in methylotrophic yeasts. *Applied*
686 *Microbiology and Biotechnology* **54**: 741–750.
687 https://doi.org/10.1007/s002530000464

688 Gupta, A., Rao, K.K., Sahu, U., and Rangarajan, P.N. (2021) Characterization of the
689 transactivation and nuclear localization functions of *Pichia pastoris* zinc finger
690 transcription factor Mxr1p. *Journal of Biological Chemistry* **297:** 101247.
691 https://doi.org/10.1016/j.jbc.2021.101247

692 Hartner, F.S. and Glieder, A. (2006) Regulation of methanol utilisation pathway genes
693 in yeasts. *Microbial Cell Factories* **5**: 1–21. https://doi.org/10.1186/1475-2859-5-39

694 Kalender, Ö. and Çalık, P. (2020) Transcriptional regulatory proteins in central carbon
695 metabolism of *Pichia pastoris* and *Saccharomyces cerevisiae*. *Applied Microbiology*
696 *and Biotechnology* **104**: 7273–7311. https://doi.org/10.1007/s00253-020-10680-2

697 Kawaguchi, K., Yurimoto, H., Oku, M., and Sakai, Y. (2011) Yeast methylotrophy and
698 autophagy in a methanol-oscillating environment on growing *Arabidopsis thaliana*
699 leaves. *PLoS ONE* **6:** e25257. https://doi.org/10.1371/journal.pone.0025257

700 van der Klei, I.J., Yurimoto, H., Sakai, Y., and Veenhuis, M. (2006) The significance of
701 peroxisomes in methanol metabolism in methylotrophic yeast. *Biochimica et*

Biophysica Acta - Molecular Cell Research **1763**: 1453–1462. https://doi.org/10.1016/j.bbamcr.2006.07.016

Leão-Helder, A.N., Krikken, A.M., Klei, I.J. Van der, Kiel, J.A.K.W., and Veenhuis, M. (2003) Transcriptional down-regulation of peroxisome numbers affects selective peroxisome degradation in *Hansenula polymorpha*. *Journal of Biological Chemistry* **278:** 40749–40756. https://doi.org/10.1074/jbc.M304029200

Levin, D. (2005) Cell wall integrity signaling in *Saccharomyces cerevisiae*. *Microbiology and Molecular Biology Reviews* **69:** 262–291. https://doi.org/10.1128/MMBR.69.2.262

Lin-Cereghino, G.P., Godfrey, L., la Cruz, B.J. de, Johnson, S., Khuongsathiene, S., Tolstorukov, I., *et al.* (2006) Mxr1p, a Key Regulator of the methanol utilization pathway and peroxisomal genes in *Pichia pastoris*. *Molecular and Cellular Biology* **26**: 883–897. https://doi.org/10.1128/mcb.26.3.883-897.2006

Madaule, P., Axel, R., and Myers, A.M. (1987) Characterization of two members of the rho gene family from the yeast *Saccharomyces cerevisiae*. *Proceedings of the National Academy of Sciences of the United States of America* **84**: 779–783. https://doi.org/10.1073/pnas.84.3.779

Nonaka, H., Tanaka, K., Hirano, H., Fujiwara, T., Kohno, H., Umikawa, M., *et al.* (1995) A downstream target of RHO1 small GTP-binding protein is PKC1, a homolog of protein kinase C, which leads to activation of the MAP kinase cascade in *Saccharomyces cerevisiae*. *EMBO Journal* **14**: 5931–5938. https://doi.org/10.1002/j.1460-2075.1995.tb00281.x

Oda, S., Yurimoto, H., Nitta, N., and Sakai, Y. (2016) Unique C-terminal region of Hap3 is required for methanol-regulated gene expression in the methylotrophic yeast *Candida boidinii*. *Microbiology* **162:** 898–907. https://doi.org/10.1099/mic.0.000275

Oda, S., Yurimoto, H., Nitta, N., Sasano, Y., and Sakai, Y. (2015) Molecular characterization of hap complex components responsible for methanol-inducible gene expression in the methylotrophic yeast *Candida boidinii*. *Eukaryotic Cell* **14:** 278–285. https://doi.org/10.1128/EC.00285-14

Ogata, K., Nishikawa, H., and Ohsugi, M. (1969) A yeast capable of utilizing methanol. *Agricultural and Biological Chemistry* **33**: 1519–1520. https://doi.org/10.1080/00021369.1969.10859497

Ohsawa, S., Inoue, K., Isoda, T., Oku, M., Yurimoto, H., & Sakai, Y. (2021) The methanol sensor Wsc1 and MAP kinase suppress degradation of methanol-induced peroxisomes in methylotrophic yeast. *Journal of Cell Science*, **134**: jcs.254714. https://doi.org/10.1242/jcs.254714

Ohsawa, S., Nishida, S., Oku, M., Sakai, Y., and Yurimoto, H. (2018) Ethanol represses the expression of methanol-inducible genes via acetyl-CoA synthesis in the yeast *Komagataella phaffii*. *Scientific Reports* **8**: 1–11. https://doi.org/10.1038/s41598-018-36732-2

Ohsawa, S., Yurimoto, H., and Sakai, Y. (2017) Novel function of Wsc proteins as a methanol-sensing machinery in the yeast *Pichia pastoris*. *Molecular Microbiology* **104**: 349–363. https://doi.org/10.1111/mmi.13631

Parua, P.K., Ryan, P.M., Trang, K., and Young, E.T. (2012) *Pichia pastoris* 14-3-3 regulates transcriptional activity of the methanol inducible transcription factor Mxr1

747 by direct interaction. *Molecular Microbiology* **85**: 282–298.
748 https://doi.org/10.1111/j.1365-2958.2012.08112.x.
749 Ratnakumar, S., Kacherovsky, N., Arms, E., and Young, E.T. (2009) Snf1 controls the
750 activity of Adr1 through dephosphorylation of Ser230. *Genetics* **182:** 735–745.
751 https://doi.org/10.1534/genetics.109.103432
752 Sahu, U., Krishna Rao, K., and Rangarajan, P.N. (2014) Trm1p, a $Zn(II)_2Cys_6$-type
753 transcription factor, is essential for the transcriptional activation of genes of
754 methanol utilization pathway, in *Pichia pastoris*. *Biochemical and Biophysical*
755 *Research Communications* **451:** 158–164. https://doi.org/10.1016/j.bbrc.2014.07.094
756 Sasano, Y., Yurimoto, H., Kuriyama, M., and Sakai, Y. (2010) Trm2p-dependent
757 derepression is essential for methanol-specific gene activation in the methylotrophic
758 yeast *Candida boidinii*. *FEMS Yeast Research* **10**: 535–544.
759 https://doi.org/10.1111/j.1567-1364.2010.00640.x
760 Sasano, Y., Yurimoto, H., Yanaka, M., and Sakai, Y. (2008) Trm1p, a $Zn(II)_2Cys_6$-type
761 transcription factor, is a master regulator of methanol-specific gene activation in the
762 methylotrophic yeast *Candida boidinii*. *Eukaryotic Cell* **7:** 527–536.
763 https://doi.org/10.1128/EC.00403-07
764 Shen, W., Kong, C., Xue, Y., Liu, Y., Cai, M., Zhang, Y., et al. (2016) Kinase screening
765 in *Pichia pastoris* identified promising targets involved in cell growth and alcohol
766 oxidase 1 promoter (P_{AOX1}) regulation. *PLoS ONE* **11:** e0167766.
767 https://doi.org/10.1371/journal.pone.0167766
768 Wang, X., Wang, Q., Wang, J., Bai, P., Shi, L., Shen, W., et al. (2016) Mit1
769 transcription factor mediates methanol signaling and regulates the alcohol oxidase 1

(*AOX1*) promoter in *Pichia pastoris*. *Journal of Biological Chemistry* **291:** 6245–6261. https://doi.org/10.1074/jbc.M115.692053

Yashar, B., Irie, K., Printen, J.A., Stevenson, B.J., Sprague, G.F., Matsumoto, K., and Errede, B. (1995) Yeast MEK-dependent signal transduction: response thresholds and parameters affecting fidelity. *Molecular and Cellular Biology* **15**: 6545–6553. https://doi.org/10.1128/mcb.15.12.6545

Young, E.T., Dombek, K.M., Tachibana, C., and Ideker, T. (2003) Multiple pathways are co-regulated by the protein kinase Snf1 and the transcription factors Adr1 and Cat8. *Journal of Biological Chemistry* **278:** 26146–26158. https://doi.org/10.1074/jbc.M301981200

Yurimoto, H. (2009) Molecular basis of methanol-inducible gene expression and its application in the methylotrophic yeast *Candida boidinii*. *Bioscience, Biotechnology and Biochemistry* **73**: 793–800. https://doi.org/10.1271/bbb.80825

Yurimoto, H., Oku, M., and Sakai, Y. (2011) Yeast methylotrophy: Metabolism, gene regulation and peroxisome homeostasis. *International Journal of Microbiology* 1–8. https://doi.org/10.1155/2011/101298

Yurimoto, H. and Sakai, Y. (2019) Methylotrophic yeasts: Current understanding of their C1-metabolism and its regulation by sensing methanol for survival on plant leaves. *Current Issues in Molecular Biology* **33**: 197–209. https://doi.org/10.21775/CIMB.033.197

792 **FIGURE LEGENDS**

793

794 **FIGURE 1** Involvement of KpMxr1 in the CRMI and phosphorylation of KpMxr1.
795 (a) Transcript levels of methanol-induced genes, *AOX1* and *DAS1,* and transcription
796 factor genes, *KpMIT1* and *KpMXR1*. Total mRNA was prepared from wild-type cells
797 cultured on various methanol concentrations (0, 0.01, 0.1, 1%) for 2 h. The transcript
798 levels were normalized using *GAP* gene as the standard. Relative transcript levels
799 compared to that of the glucose pre-cultured sample are indicated. Error bars represent
800 standard error values from three independent experiments. (b) Transcript levels of
801 *AOX1* and *DAS1* in *Kpmxr1Δ* (white bars), *Kpmit1Δ* (light grey bars), *Kptrm1Δ* (dark
802 grey bars) and *Kphap3Δ* (black bars) strains. Total mRNA was prepared from cells of
803 each strain cultured under various methanol concentrations (0, 0.01, 0.1, 1%) for 2 h.
804 The transcript levels were normalized using *GAP* gene as the standard. The strains used
805 in this experiment and the mean value of relative transcript levels are indicated in left
806 side of the graphs. Relative transcript levels compared to that of the glucose pre-
807 cultured sample are also presented. Error bars represent standard error values from three
808 independent experiments. (c) Immunoblot analysis of KpMxr1-FLAG protein level in
809 response to varying methanol concentrations (α-FLAG). Actin was blotted as a loading
810 control (α-Actin). Cells were shifted from glucose medium (SD) to medium with
811 indicated methanol concentration (SM) for 30 min. Molecular weights of each band
812 calculated from the protein size marker are indicated. The groups indicated with
813 different symbol means significant difference (between a and b, *: $p < 0.05$) by the
814 statistical analysis (One-way ANOVA) (d) Phosphorylation levels of KpMxr1-FLAG in
815 response to varying methanol concentrations. SD, 2% glucose medium; SM, 0, 0.01,
816 0.1, or 1% methanol media. KpMxr1-FLAG in whole cell extracts was detected in an
817 input sample with anti-FLAG antibody (α-FLAG), and actin was blotted as a loading
818 control (α-Actin). KpMxr1-FLAG was immunoprecipitated with anti-FLAG antibody

819 (IP), and phosphorylation of KpMxr1-FLAG was detected with anti-phosphoserine (α-
820 P-serine), anti-phosphothreonine (α-P-threonine) or anti-phosphotyrosine (α-P-tyrosine)
821 antibodies (IB). Cells were shifted from glucose medium (SD) to medium with
822 indicated methanol concentrations (SM) for 30 minutes. Molecular weights of each
823 band calculated from the protein size marker are indicated.
824

825 **FIGURE 2** Functional and phosphorylation analyses of truncated KpMxr1 proteins.
826 (a) Construction of C-terminal truncated KpMxr1 mutant proteins. (b) Transcript levels
827 of *AOX1* in strains expressing the full-length KpMxr1^{FL} protein (FL1155) (white bars),
828 KpMxr1$^{1-525}$ (TM525) (white bars with diagonal line), KpMxr1$^{1-368}$ (TM368) (grey
829 bars), KpMxr1$^{1-230}$ (TM230) (grey bars with diagonal line) and KpMxr1$^{1-211}$ (TM211)
830 (black bars). Total mRNA was prepared from cells of each strain cultured on various
831 concentrations of methanol (0, 0.01, 0.1, 1%) for 2 h. The transcript levels were
832 normalized using *GAP* gene as the standard. Relative transcript levels compared to that
833 of the glucose pre-cultured sample are also presented. Error bars represent standard
834 error values from three independent experiments. *: $p < 0.05$, n.s.: not significant
835 (c) Growth of strains expressing truncated KpMxr1 proteins on methanol. Strains
836 expressing KpMxr1^{FL} (filled squares), KpMxr1$^{1-525}$ (open squares), KpMxr1$^{1-368}$ (filled
837 circles), KpMxr1$^{1-230}$ (open circles) and KpMxr1$^{1-211}$ (filled triangles) and the *Kpmxr1Δ*
838 strain (open triangles) were grown on 0.5% methanol medium (SM). (d)
839 Phosphorylation levels of truncated KpMxr1-FLAG proteins. Cells were grown on
840 glucose (SD) and shifted to 0.1% methanol (SM) medium for 30 min. C-terminal
841 FLAG-tagged KpMxr1$^{1-525}$, KpMxr1$^{1-368}$ and KpMxr1$^{1-230}$ were immunoprecipitated
842 with FLAG antibody and treated with or without λ-phosphatase (λ-Ppase). The samples
843 were loaded on an 8.5% acrylamide SDS-PAGE gel with or without 20 μM phos-tag,
844 and transferred to a PVDF membrane, and the truncated KpMxr1-FLAG proteins were
845 detected with an anti-FLAG antibody. The protein size marker and molecular weights of
846 each band calculated from the protein size marker are indicated. Black arrowheads
847 correspond to the bands of phosphorylated KpMxr1 protein. (e) Phosphorylation level
848 of KpMxr1$^{1-230}$-FLAG protein based on methanol concentration. Cells were shifted

849 from glucose medium (SD) to medium with indicated methanol concentration for 30
850 min. KpMxr1$^{1\text{-}230}$-FLAG was immunoprecipitated with FLAG antibody and subjected
851 to phos-tag analyses as described in (d). The protein size marker and molecular weights
852 of each band calculated from the protein size marker are indicated. Black arrowheads
853 correspond to the detected bands of phosphorylated KpMxr1 protein.

FIGURE 3 Identification of KpMxr1 phosphorylation sites related to the regulation of the CRMI. (a) LC–MS/MS analysis of KpMxr1 phosphorylation. Cells of TM525 strain cultured in glucose (2%) or methanol (0.1%) media for 30 min were lysed and KpMxr1$^{1\text{-}525}$-FLAG protein was immunoprecipitated with anti-FLAG antibody. Obtained samples were loaded on a 7.5% acrylamide SDS-PAGE gel and stained with CBB. The target band was cut out and treated with Trypsin. The sum values of detected peak intensity of LC-MS/MS obtained from glucose-cultured samples (white bars) and methanol-cultured samples (black bars) are indicated. Asterisks mean mutated serine and threonine residues in SA and TA mutant proteins. (b) Transcript levels of *AOX1* in the control strain expressing KpMxr1^{FL}-FLAG (white bars), strain MSA expressing KpMxr1^{FL}-SA-FLAG (grey bars) and strain MTA expressing KpMxr1^{FL}-TA-FLAG (black bars). Total mRNAs were prepared from cells of each strain cultured on various concentrations of methanol (0, 0.01, 0.03, 0.1, 1%) for 2 h. The transcript levels were normalized using *GAP* gene as the standard. Relative transcript levels compared to that of the glucose pre-cultured sample are indicated. Error bars represent standard error values from three independent experiments. (c) Phosphorylation levels of KpMxr1$^{1\text{-}230}$-FLAG (WT), KpMxr1$^{1\text{-}230}$SA-FLAG (SA) and KpMxr1$^{1\text{-}230}$TA-FLAG (TA) proteins. Cells were grown on glucose (SD) and shifted to 0.1% methanol (SM) medium for 30 min. C-terminal FLAG-tagged KpMxr1$^{1\text{-}230}$, KpMxr1$^{1\text{-}230}$SA and KpMxr1$^{1\text{-}230}$TA were immunoprecipitated with FLAG antibody, and treated with or without λ-phosphatase (λ-Ppase). The samples were loaded on an 8.5% acrylamide SDS-PAGE gel with or without 20 μM phos-tag, and transferred to a PVDF membrane, and truncated KpMxr1-FLAG proteins were detected with anti-FLAG antibody. The black arrowhead indicates the band which is lost in the SA samples from glucose-grown cells.

878 The protein size marker and molecular weights of each band calculated from the protein
879 size marker are indicated.

FIGURE 4 Effects of expression of wild-type and hyperactive mutants of KpRho1-Myc, KpPkc1-HA and KpMkk1-HA in the control strain (+E.V.) on KpMpk1 phosphorylation and *AOX1* transcript level. (a-c) Upper panels, immunoblot analysis of expressed proteins detected with anti-Myc antibody or anti-HA antibody, and phosphorylated KpMpk1 (P-Mpk1) detected with anti-phosphor-Mpk1 antibody. Lower panels, transcript levels of *AOX1*. Total mRNA was prepared from the cells of each strain cultured in 0.01% methanol media without (white bars) or with 50 μM $CuSO_4$ (black bars) for 2 h. The transcript levels were normalized using *GAP* gene as the standard. Relative transcript levels compared to that of the control strain without $CuSO_4$ are indicated. Error bars represent standard error values from three independent experiments. Molecular weights of each band calculated from the protein size marker are indicated. *: $p < 0.05$, n.s.: not significant (a) The strain expressing KpRho1-Myc and the strain expressing KpRho1^{Q68H}-Myc; (b) the strain expressing KpPkc1-HA and the strain expressing KpPkc1^{R390P} -HA; (c) the strain expressing KpMkk1-HA and the strain KpMkk1^{S313P}-HA under the control of the *ScCUP1* promoter. (d) Transcript levels of *AOX1* in the *Kpmxr1Δ, Kpmit1Δ, Kptrm1Δ, Kphap3Δ, Kpmig1Δ* and *Kprop1Δ* strains expressing KpRho1^{Q68H} under the control of the *ScCUP1* promoter. Total mRNA was prepared from the cells of each strain cultured in 0.01% methanol media without (white bars) or with 50 μM $CuSO_4$ (black bars) for 2 h. The transcript levels were normalized using *GAP* gene as the standard. Relative transcript levels compared to that of the control strain without $CuSO_4$ are indicated. Error bars represent standard error values from three independent experiments.

FIGURE 5 Effects of the hyperactive mutation KpPkc1^{R390P} on KpMxr1-phosphorylation and *AOX1* transcript level. (a) Phosphorylation level of KpMxr1$^{1-230}$-FLAG detected with phos-tag immunoblot analysis using the strain expressing KpPkc1^{R390P}-HA under the control of the *ScCUP1* promoter. Protein samples were prepared from the cells cultured in 0.1% methanol media with or without $CuSO_4$ 50 μM for 30 min. (Left panel) KpMxr1$^{1-230}$-FLAG expression under the original promoter and KpPkc1^{R390P}-HA under the *ScCUP1* promoter in whole cell extracts was detected in input samples with anti-FLAG antibody, anti-HA antibody and anti-actin antibody, respectively. (Right panel) KpMxr1$^{1-230}$-FLAG was immunoprecipitated with FLAG antibody. The samples were treated with or without λ-phosphatase (λ-Ppase), loaded on an 8.5% acrylamide SDS-PAGE gel with 20 μM or without phos-tag, and transferred to a PVDF membrane, and detected with an anti-FLAG antibody. The protein size marker and molecular weights of each band calculated from the protein size marker are indicated. Black arrowhead corresponds to the detected bands of phosphorylated KpMxr1 protein. (b) Immunoblot analysis of KpMxr1-FLAG, Pkc1^{R390P}-HA, phosphorylated KpMpk1 and β-actin in the strain expressing KpPkc1^{R390P} under the control of the *ScCUP1* promoter. Cells were grown on glucose and shifted to methanol (SM) medium for 2 h at various concentrations of Cu^{2+}. The lysed samples were subjected to immunoblot analysis. Molecular weights of each band calculated from the protein size marker are indicated. Phosphorylation of KpMpk1 was detected with anti-phosphor-Mpk1 antibody (P-Mpk1). (c) Transcript levels of *AOX1* in the strain expressing KpPkc1^{R390P} under the control of the *ScCUP1* promoter. Total mRNA was prepared from cells cultured on methanol containing various concentrations of $CuSO_4$ (0, 1, 10, 50, 100 μM) for 2 h. The transcript levels were normalized using *GAP* gene as

927 the standard. Relative transcript levels compared to that of the glucose pre-cultured
928 sample are indicated. Error bars represent standard error values from three independent
929 experiments.
930
931

FIGURE 6 Regulatory model of CRMI. The phosphorylation state of KpMxr1 is controlled by the CRMI pathway including KpWsc1/KpWsc3 (Wsc), KpRom2, KpRho1 and KpPkc1. The methanol signal according to methanol concentration is transmitted from this pathway to KpMxr1 independent of the MAPK cascade, which inhibits pexophagy under high methanol condition (pexophagy-repression pathway). The serine residues (including S110/S111) in KpMxr1 are dephosphorylated by the medium shift from glucose to methanol, while the threonine residues are phosphorylated by the same medium shift. Multiple serine and threonine residues are phosphorylated in various patterns based on the methanol concentration. KpPkc1 regulates the phosphorylation status of KpMxr1 corresponding to methanol concentration. The active form of KpPkc1 increases depending on methanol concentration. The middle level of KpPkc1 activity (light gray) make KpMxr1 most active form (dark gray), but the high level of KpPkc1 activity (dark gray) phosphorylates serine residues (including S110/S111) and dephosphorylates threonine residues of KpMxr1 to repress methanol-induced gene expression. This phosphoregulation of KpMxr1 plays a critical role in maintaining the appropriate level of expression of methanol-induced genes.

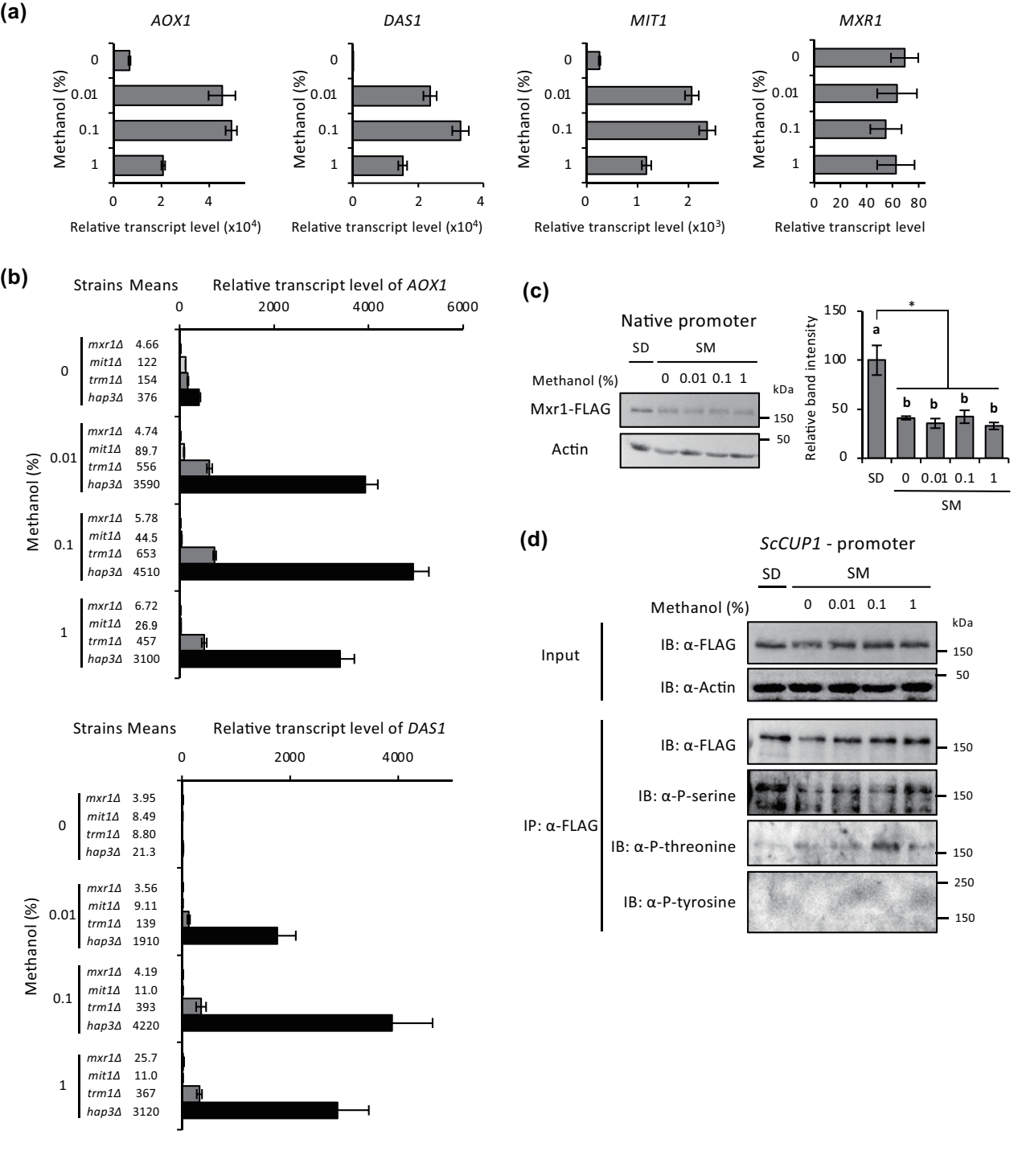
(a)
AOX1
DAS1
MIT1
MXR1
Methanol (%)
0
0.01
0.1
1
Relative transcript level (x10^4)
Relative transcript level (x10^4)
Relative transcript level (x10^3)
Relative transcript level
(b)
Strains Means
Relative transcript level of AOX1
mxr1Δ 4.66
mit1Δ 122
trm1Δ 154
hap3Δ 376
mxr1Δ 4.74
mit1Δ 89.7
trm1Δ 556
hap3Δ 3590
mxr1Δ 5.78
mit1Δ 44.5
trm1Δ 653
hap3Δ 4510
mxr1Δ 6.72
mit1Δ 26.9
trm1Δ 457
hap3Δ 3100
Strains Means
Relative transcript level of DAS1
mxr1Δ 3.95
mit1Δ 8.49
trm1Δ 8.80
hap3Δ 21.3
mxr1Δ 3.56
mit1Δ 9.11
trm1Δ 139
hap3Δ 1910
mxr1Δ 4.19
mit1Δ 11.0
trm1Δ 393
hap3Δ 4220
mxr1Δ 25.7
mit1Δ 11.0
trm1Δ 367
hap3Δ 3120
(c)
Native promoter
SD
SM
Methanol (%)
0 0.01 0.1 1
kDa
Mxr1-FLAG
Actin
150
50
Relative band intensity
a
b
SD
0 0.01 0.1 1
SM
(d)
ScCUP1 - promoter
SD
SM
Methanol (%)
0 0.01 0.1 1
kDa
Input
IB: α-FLAG
IB: α-Actin
IP: α-FLAG
IB: α-FLAG
IB: α-P-serine
IB: α-P-threonine
IB: α-P-tyrosine
150
50
250

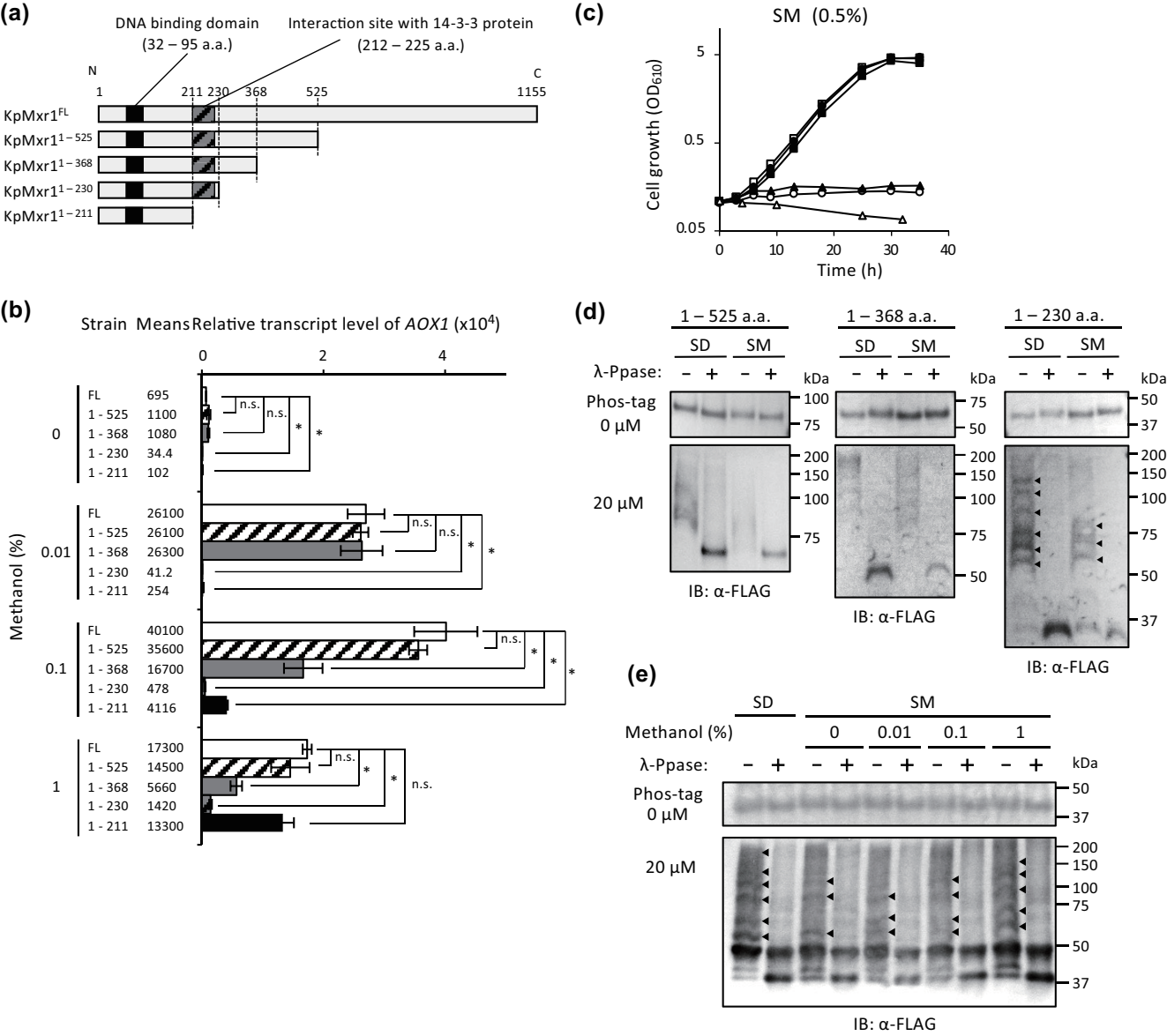
(a)
DNA binding domain
(32 – 95 a.a.)
Interaction site with 14-3-3 protein
(212 – 225 a.a.)
N
C
1
211 230
368
525
1155
KpMxr1FL
KpMxr1 1 – 525
KpMxr1 1 – 368
KpMxr1 1 – 230
KpMxr1 1 – 211
(b)
Strain Means
Relative transcript level of AOX1 (x10^4)
0
2
4
Methanol (%)
0
FL 695
1 - 525 1100
1 - 368 1080
1 - 230 34.4
1 - 211 102
0.01
FL 26100
1 - 525 26100
1 - 368 26300
1 - 230 41.2
1 - 211 254
0.1
FL 40100
1 - 525 35600
1 - 368 16700
1 - 230 478
1 - 211 4116
1
FL 17300
1 - 525 14500
1 - 368 5660
1 - 230 1420
1 - 211 13300
n.s.
*
(c)
SM (0.5%)
Cell growth (OD610)
5
0.5
0.05
0
10
20
30
40
Time (h)
(d)
1 – 525 a.a.
1 – 368 a.a.
1 – 230 a.a.
SD
SM
λ-Ppase:
kDa
Phos-tag
0 μM
20 μM
100
75
50
37
200
150
IB: α-FLAG
(e)
SD
SM
Methanol (%)
0
0.01
0.1
1
λ-Ppase:
kDa
Phos-tag
0 μM
20 μM
50
37
200
150
100
75
IB: α-FLAG

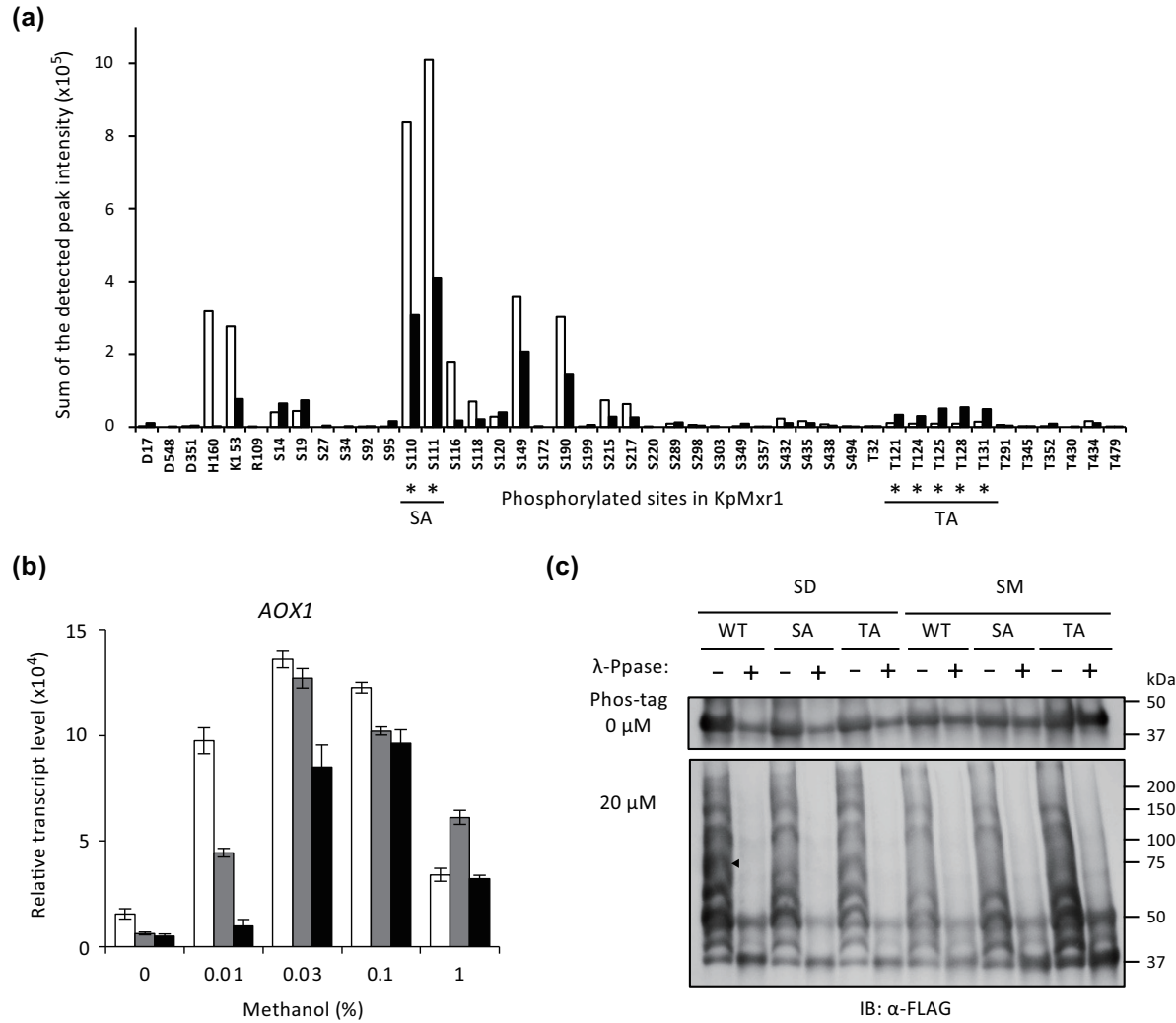
(a)
Sum of the detected peak intensity (x10^5)
10
8
6
4
2
0
D17 D548 D351 H160 K1 53 R109 S14 S19 S27 S34 S92 S95 S110 S111 S116 S118 S120 S149 S172 S190 S199 S215 S217 S220 S289 S298 S303 S349 S357 S432 S435 S438 S494 T32 T121 T124 T125 T128 T131 T291 T345 T352 T430 T434 T479
* *
SA
Phosphorylated sites in KpMxr1
* * * * *
TA
(b)
AOX1
Relative transcript level (x10^4)
15
10
5
0
0
0.01
0.03
0.1
1
Methanol (%)
(c)
SD
SM
WT SA TA WT SA TA
λ-Ppase: – + – + – + – + – + – +
kDa
Phos-tag
0 μM
20 μM
50
37
200
150
100
75
50
37
IB: α-FLAG

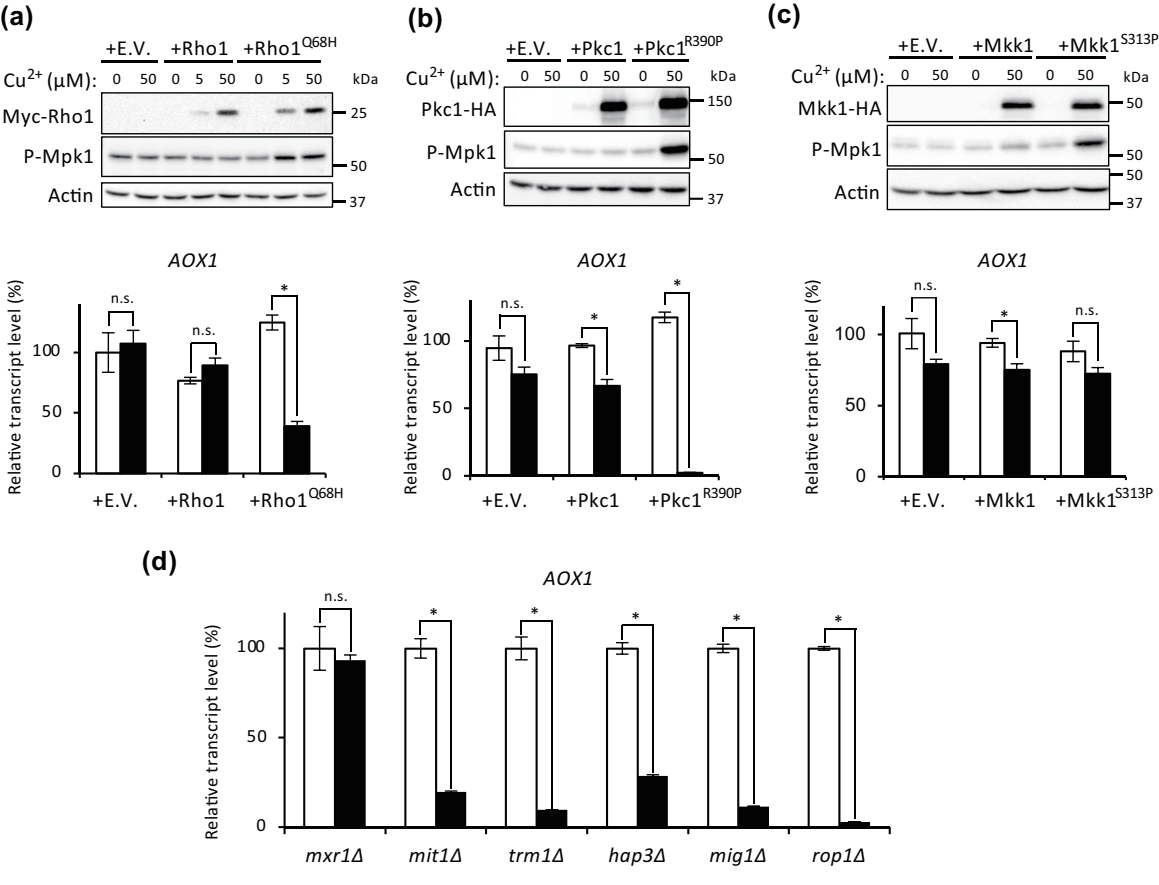
(a)
+E.V.
+Rho1
+Rho1Q68H
Cu2+ (μM):
0 50 0 5 50 0 5 50
kDa
Myc-Rho1
P-Mpk1
Actin
25
50
37
AOX1
Relative transcript level (%)
n.s.
n.s.
*
100
50
0
+E.V.
+Rho1
+Rho1Q68H
(b)
+E.V.
+Pkc1
+Pkc1R390P
Cu2+ (μM):
0 50 0 50 0 50
kDa
Pkc1-HA
P-Mpk1
Actin
150
50
37
AOX1
Relative transcript level (%)
n.s.
*
*
100
50
0
+E.V.
+Pkc1
+Pkc1R390P
(c)
+E.V.
+Mkk1
+Mkk1S313P
Cu2+ (μM):
0 50 0 50 0 50
kDa
Mkk1-HA
P-Mpk1
Actin
50
50
50
37
AOX1
Relative transcript level (%)
n.s.
*
n.s.
100
50
0
+E.V.
+Mkk1
+Mkk1S313P
(d)
AOX1
Relative transcript level (%)
n.s.
*
*
*
*
*
100
50
0
mxr1Δ
mit1Δ
trm1Δ
hap3Δ
mig1Δ
rop1Δ

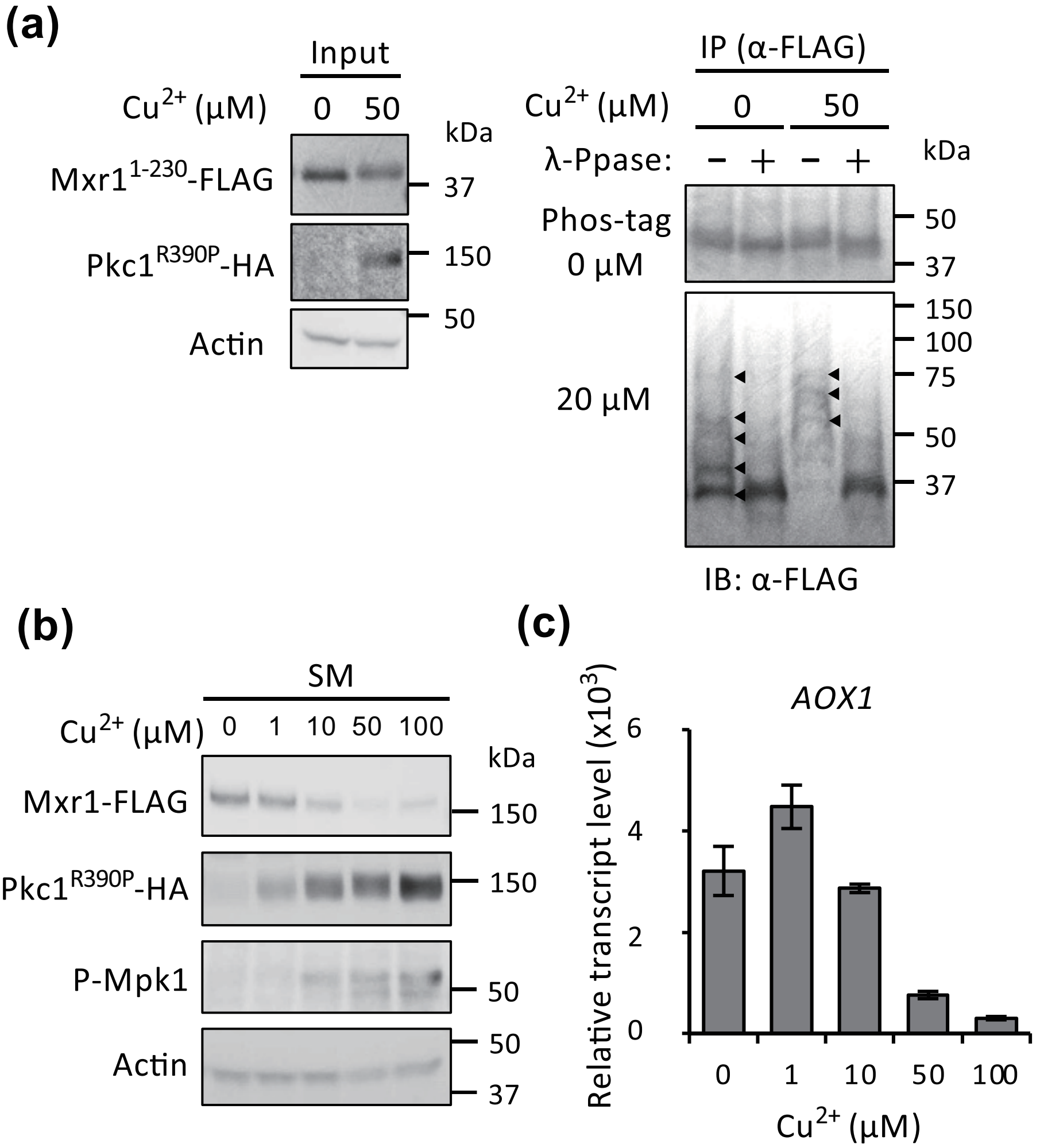
(a)
Input
Cu2+ (μM) 0 50
kDa
Mxr1 1-230 -FLAG
37
Pkc1 R390P -HA
150
50
Actin
IP (α-FLAG)
Cu2+ (μM) 0 50
λ-Ppase: − + − +
kDa
Phos-tag
0 μM
50
37
150
100
75
20 μM
50
37
IB: α-FLAG
(b)
SM
Cu2+ (μM) 0 1 10 50 100
kDa
Mxr1-FLAG
150
Pkc1 R390P -HA
150
P-Mpk1
50
Actin
50
37
(c)
AOX1
Relative transcript level (x10 3)
6
4
2
0
0 1 10 50 100
Cu2+ (μM)

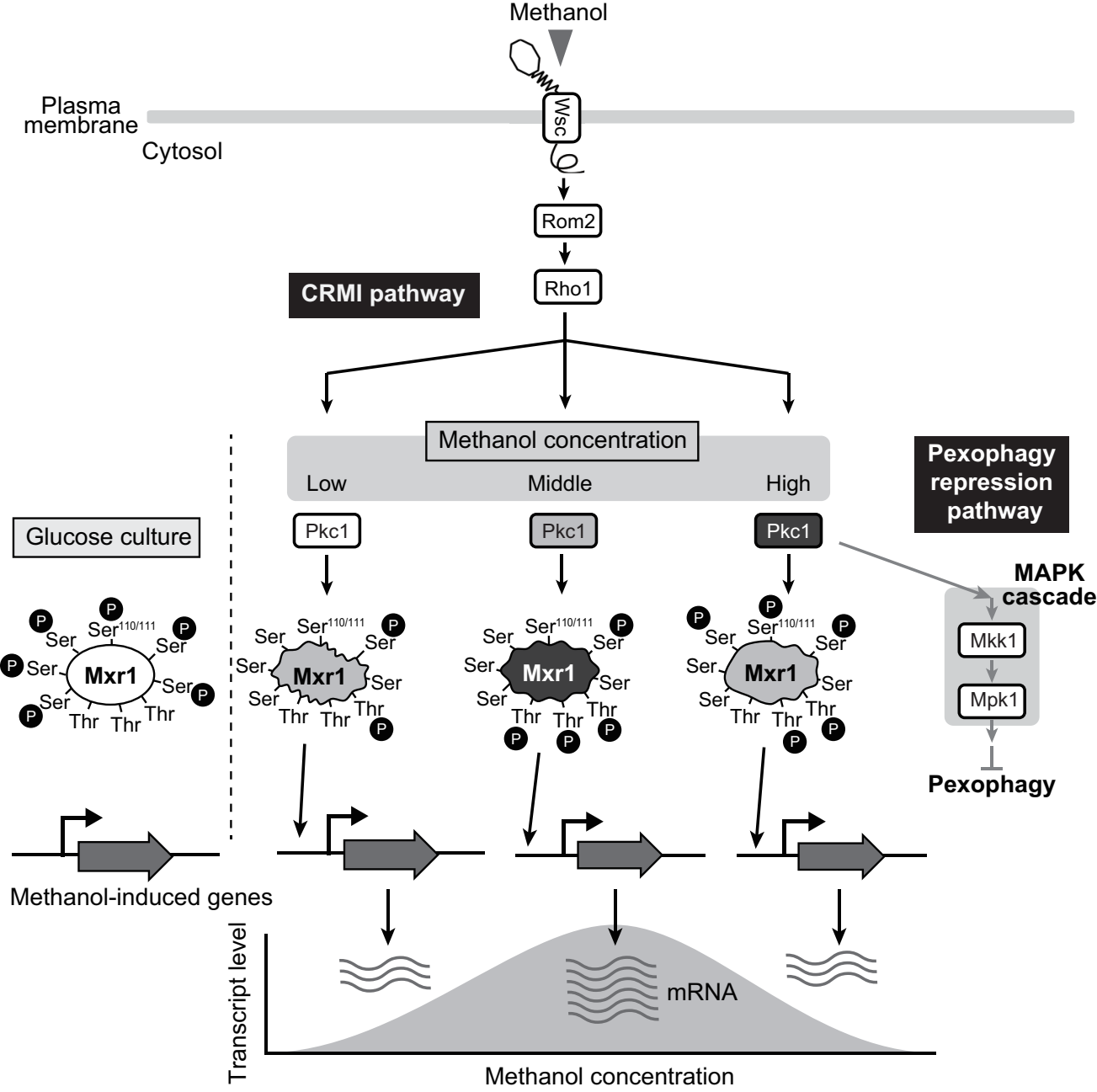
Methanol
Plasma membrane
Cytosol
Wsc
Rom2
Rho1
CRMI pathway
Methanol concentration
Low
Middle
High
Pexophagy repression pathway
Glucose culture
Pkc1
Pkc1
Pkc1
MAPK cascade
Mkk1
Mpk1
Pexophagy
Mxr1
Mxr1
Mxr1
Methanol-induced genes
Transcript level
mRNA
Methanol concentration